THE OBSERVATORY

Vol. 144 | 2024 FEBRUARY | No. 1298

ESTIMATION OF VISUAL-BINARY ORBITAL ELEMENTS UTILIZING OPTIMAL CURVE-FITTING PROCEDURES

By M. D. Rhodes[1]*, T. S. Banks*[2]*, E. Budding*[3] *& T. Love*[4]
[1]*Brigham Young University, Utah, USA*
[2]*Dept. of Physical Science & Engineering, Harper College, USA*
[3]*Carter Observatory, Wellington, New Zealand*
[4]*Variable Stars South, Wellington, New Zealand*

We demonstrate optimal curve-fitting procedures to the parametrization of a selection of 25 visual-binary-star orbits from F. W. Dyson's[1] catalogue. We compare our findings with other published results, which reveal uncertainties, real and formal, affecting the parameters. The extent of data coverage for any one system can have a substantial impact on the modelled results, with various orbital solutions sometimes possible for a single system.

Introduction

Comparative study of the properties of binary stars started in the late-18th Century, notably with the work of the Herschel family. In his classic review of wide double stars, W. Herschel[2] was able to confirm Newtonian gravity as the agent for their apparent motions in Keplerian ellipses. Visual binaries at known distances are thus able to reveal useful physical characteristics of stars, namely their masses and luminosities. However, the proportion of visual binaries for which elliptic orbital motion was clearly established has been low, usually involving periods of up to just a few hundred years, *i.e.*, separations of a few score AU.

Background

To scale the observed angular separation on the sky of the two components of a visual binary to absolute units, it is necessary to know the system's mean parallax. Historically, this was difficult to derive with high accuracy, even for the nearest stars[3–5]. This point has limited the extent to which the astrometry of visual pairs could bear on general astrophysics until relatively recent times. Even though there may be a few-hundred binaries with parallaxes greater than 0·1 arcsec, such is the increase in numbers of stars of low mass that ~90% of this nearby population would be made up of stars with less than half the mass of the Sun. Increased precision of double-star data, including parallaxes, obtained from modern space-based platforms is likely to change this perspective considerably over coming years[6]. The present juncture offers opportunities to look back over historical data and check on methods for accurate parametrization of datasets.

The elliptical form of an orbit is written in the standard arrangement as given by Smart[7]:

$$Ax^2 + 2Hxy + By^2 + 2Gx + 2Fy + 1 = 0. \qquad (1)$$

The essence of the inverse problem for the visual-binary orbit is to relate the five coefficients A–H to the five regular orbital parameters a, e, i, ω, and Ω. The values of A–H can be derived from an appropriate selection of x and y values on the observed ellipse. Meanwhile, the orbital parameters in their own natural frame of reference (ξ, η) of reference, centred on the primary focus, satisfy

$$\frac{(\xi + ae)^2}{a^2} + \frac{\eta^2}{a^2(1 - e^2)} = 1. \qquad (2)$$

This would correspond directly with the apparent orbit only in the 'face-on' conditions that $\Omega = \pi/2$, i and $\omega = 0$. In general, these three 'Eulerian' angles are associated with coordinate rotations about, progressively, the z, x, and z (again) axes, with the result that for a point on the orbit where the true anomaly is v, the x, y, and z (*i.e.*, line of sight) coordinates satisfy the following equations[8]:

$$x = \frac{a(1 - e^2)}{(1 + e\cos v)}[\cos(v + \omega)\sin\Omega + \sin(v + \omega)\cos\Omega\cos i],$$

$$y = \frac{a(1 - e^2)}{(1 + e\cos v)}[\cos(v + \omega)\cos\Omega - \sin(v + \omega)\sin\Omega\cos i],$$

$$z = \frac{a(1 - e^2)}{(1 + e\cos v)}\sin(v + \omega)\sin i. \qquad (3)$$

Various methods exist to relate the five constants in (1) to those in (3).

Classical methods involve reversing the three rotational coordinate transformations that gave rise to (3) from the natural, un-rotated, forms for ξ and η. The set of equations (3) is inverted to find forms for ξ and η in terms of x and y. These can be substituted into (2) and then comparison of the terms in x^2, xy, y^2, *etc.*, allow the relations between the five observationally derived coefficients A–H to be related to the parameters a–Ω. There are still the two time-related parameters that fix the position of the secondary with respect to the primary for any particular time, namely the orbital period P and reference epoch T_0. A pair of points on the ellipse, at known times, are sufficient to derive these, their true anomaly values being determined from (3) with the known geometric parameters. Both these v values have a corresponding mean anomaly, which, taken together, fix the values of P and T_0.

With the use of modern computers, it becomes easily practicable to deal with the parametrization of the fitting function by programmed optimization methods. Instead of carrying out linear operations with A–H determined from selected points on the apparent orbit, the ellipse that corresponds to (2) is progressively matched to the full x and y datasets to minimize residuals.

The fitting functions will contain the full seven constants discussed above, as well as small fiducial corrections, Δx_0, Δy_0, in the position to be assigned to the origin. Formally, we can write for the solution of the inverse problem set out in this way[9,10]:

$$\boldsymbol{a}_{\text{opt}} = [\chi^2]^{-1}\text{Min}[\chi^2(\boldsymbol{a})], \tag{4}$$

where $\boldsymbol{a}_{\text{opt}}$ is the vector of best estimates of each parameter in the adjustable set $\{a_1, a_2, a_3 \ldots a_j \ldots a_m\}$. The observed values of the variable, either x or y, or both, are matched by the values of the fitting function, calculated from (3). The z values, that may be available in certain cases, can be treated in the same way.

The quantity χ^2 depends on the squared differences of observed and calculated quantities, and the optimal estimate for each a_j is taken to occur when χ^2 is minimized. The quantity $[\chi^2]^{-1}$ expresses the idea of inversion of the dependence of χ^2 on $\boldsymbol{a}$. Posed in this way, parametrization of the orbit model becomes a standard optimization problem. The inversion can be regarded as a guided trial-and-error process, in which exploration of the (χ^2, $\boldsymbol{a}$) hypersurface locates the appropriate minimum. The search direction is optimized by its alignment with the local gradient of the fitting function, and the extent of movement in this direction can be ascertained from a local grid-search. The well-known Levenberg–Marquardt procedure carries out these two operations in a suitably weighted combination[11]. The numerical value of the gradient ('steepest descent') applies to a short path-length in the (χ^2, $\boldsymbol{a}$) hypersurface, where we can regard the fitting function as the application of Eqns (3) to match the observations of the separation and position angle. This is effectively linearized as the leading terms in the corresponding Taylor series. Linearization of the fitting function is equivalent to a parabolization of the local (χ^2, $\boldsymbol{a}$) hypersurface. This will allow that grid-searching with small steps determines both the search direction, from the available conjugate axes of local (χ^2, $\boldsymbol{a}$) elliptical contours, and the distance to travel in that direction, *i.e.*, to the centre of such a contour[12].

This is essentially the approach of Bevington's[13] CHIFIT program, where the position of, and direction to, the optimum are calculated from the behaviour of χ^2 in response to parameter variation. Convergence implies a Newton–Raphson closeness of priors to their posterior counterparts. This method has been implemented by the authors as FitAstrometry.

FitAstrometry is thus an inherently iterative procedure, continuing until fit improvements have fallen below a pre-set small quantity, if that happens before a pre-set maximum number of iterations. After each fourth iteration, in the current version, conjugate-axis and centring calculations are carried out to locate the current estimate of the Min(χ^2, $\boldsymbol{a}$) position. This combination of grid-search and elliptical contour fixing are usually productive for rapid orbit model parametrization. But occasionally we have the 'long valley' problem where a group of parameters are close to linear correlation, and the trend of model improvements becomes slow, or ineffective. An example of this was found in modelling the orbit of 36 And (WDS 00550+2338). This application is discussed below. The general usefulness of modelling procedures is circumscribed by the extent and accuracy of the orbital data. Uncertainties in the parametrization arise with observational scatter and limited coverage of the orbit.

Our main purposes in what follows are (i) to demonstrate optimal curve-fitting procedures to the parametrization of a selection of visual-binary-star orbits from Dyson's catalogue; and (*ii*) to compare findings with other published results. This should reveal uncertainties, real and formal, affecting the parameters. Consequently, (*iii*) we offer updated quantities of physical interest. FitAstrometry is now an option in WinFitter and freely available to researchers. Further information is given by Budding & Demircan.[14]

Selection of data and method

The work of Dyson and his colleagues[1] published in the section titled *Orbits of 25 Double Stars* represents a fairly complete and homogeneous data set. The observations span an interval from the early 1800s to 1921. Twenty-three orbit models were published by Jackson[15]. The system 73 Oph (WDS 18096+0400) was added later and BD+18 3182 (WDS 16289+1825) was recomputed including observations from the Yerkes Observatory. Such a data set was ideal for the purpose of testing FitAstrometry, with the added advantage that we had available an additional hundred years of data (sourced from the *Washington Double Star Catalogue*[16] courtesy of the USNO) compared to Dyson. We could therefore contrast solutions based on just the Dyson data with those including the more recent data, acting as an update and hopefully a validation of Dyson's work.

Table I summarizes the values of the orbital parameters of these 25 binary stars taken from Dyson (D), the *Washington Catalogue* (W), and the optimized values from the FitAstrometry program (F).

Table II summarizes the calculated values of the dynamical parallaxes using orbital parameters of the 25 binary stars taken from Dyson (D), the *Washington Catalogue* (W), and the optimized values from the FitAstrometry program. Parallax values obtained from the *Hipparcos* and *Gaia* satellite data are shown for comparison.

Results and comparison with Dyson and WDS parameters

We ran FitAstrometry on each of the 25 Dyson visual binaries, using the full data sets including the WDS data. In Table III we present only the results of the fitting for the first system, WDS 00550+2338 (36 And). Orbital plots from Dyson, WDS, and FitAstrometry are shown in Figs. 1, 2, and 3. An appendix maintained at https://michaelrhodesbyu.weebly.com contains the FitAstrometry findings for all 25 of the Dyson (1921) collection.

The final parameter estimates for the 25 systems from WDS and FitAstrometry are in close agreement, as demonstrated by the high correlation values (see Table IV) together with the gradient of these linear models being close to unity. However, the Dyson values differ significantly from WDS and FitAstrometry values, as shown by the R^2 values for two selected parameters (i and ω). This significance was reduced by recognizing that Dyson restricted inclination values to be less than or equal to 90 degrees and that ω be less than 180 degrees. These are ambiguities rather than actual errors since ω + 180 will produce the same result as ω. Making these changes led to improved agreement between the solutions, as evidenced by the correlations shown in the column "WDS to adjusted Dyson" in Table IV. Once these adjustments were made, the agreement between WDS (and by proxy FitAstrometry) and Dyson's values is reasonable (see Figs. 4a and b), particularly given that Dyson's fits cover a shorter time period.

These systems have long periods, and in many cases Dyson's data had not covered a complete orbit. A more representative comparison against the Dyson parameter estimates is therefore to model only the data available to Dyson. Below are the results of following that procedure with the first Dyson binary, WDS 00550+2338. Table V shows the results using only the Dyson values of the orbital parameters and Table VI shows the result using the WDS values of the orbital parameters. Fig. 5 compares the orbital plots of the corresponding results.

TABLE I

A comparison of the orbital elements given in Dyson's catalogue[1] *(D), the Washington Double Star Catalogue*[16] *(W), and the FitAstrometry (F) optimized values of the 25 Dyson binary-orbit fittings. P is in Besselian years, a in arcseconds, ω, i, and Ω are in degrees, and T_0 is in decimal tropical years AD. The precision suggested by the number of digits retained after the decimal point slightly exceeds its real value.*

	P	a	e	ω	i	Ω	T_0
D-1	124·2	0·970	0·708	76·5	41·2	105·7	1816·9
W	167·4	0·984	0·306	358·6	44·6	173·7	1956·2
F	168·6	1·014	0·308	358·6	45·2	173·8	1956·3
D-2	167·4	0·974	0·313	303·7	61·3	99·7	1894·5
W	145·4	0·890	0·263	322·7	63·8	99·1	1899·1
F	145·0	0·844	0·254	326·0	60·8	99·6	1901·2
D-3	216·9	0·407	0·545	350·0	37·0	106·5	1919·4
W	522·2	0·625	0·679	238·1	157·2	13·0	1911·6
F	495·0	0·619	0·670	234·0	153·0	10·0	1912·0
D-4	95·2	0·440	0·050	174·8	58·2	55·3	1917·2
W	188·0	0·549	0·450	31·0	52·7	72·9	1887·0
F	189·0	0·568	0·430	32·0	57·0	74·0	1888·0
D-5	88·2	0·627	0·519	316·3	50·4	122·0	1882·9
W	98·0	0·743	0·592	312·3	50·3	142·6	1882·5
F	94·0	0·751	0·620	307·0	53·9	143·7	1982·0
D-6	59·6	0·350	0·611	114·9	74·6	35·2	1861·1
W	58·0	0·343	0·672	241·0	72·5	9·5	1944·2
F	57·0	0·326	0·680	236·0	69·0	7·0	1943·0
D-7	110·1	0·319	0·473	44·5	32·2	124·6	1883·6
W	104·6	0·329	0·436	33·2	19·4	132·5	1987·5
F	105·0	0·353	0·443	28·0	28·0	139·0	1987·0
D-8	361·0	1·000	0·926	59·1	43·6	78·4	1888·1
W	421·3	1·071	0·901	17·9	112·4	147·7	1892·9
F	486·0	1·130	0·909	14·0	131·0	146·0	1893·0
D-9	220·4	1·205	0·856	241·4	47·4	52·8	1860·3
W	245·0	1·111	0·833	140·0	160·0	65·0	1865·0
F	242·0	1·005	0·820	140·0	160·0	148·0	1863·0
D-10	193·6	2·549	0·460	180·5	39·4	156·3	1913·3
W	156·0	2·443	0·447	200·0	47·7	156·6	1916·7
F	157·0	2·438	0·446	199·0	47·2	155·8	1916·0

TABLE I (*concluded*)

	P	a	e	ω	i	Ω	T_0
D-11	238·0	1·060	0·700	208·6	57·6	74·1	1868·3
W	253·0	1·111	0·699	328·0	118·0	251·3	1866·0
F	250·0	1·100	0·700	327·0	117·0	251·0	1867·0
D-12	88·5	0·330	0·553	222·3	25·6	41·7	1882·6
W	89·0	0·327	0·523	171·0	165·0	71·0	2060·7
F	89·0	0·315	0·529	171·4	173·0	71·0	2061·0
D-13	234·8	1·271	0·560	23·1	40·9	174·5	1865·0
W	257·0	1·450	0·579	339·0	134·0	176·0	1894·0
F	261·0	1·466	0·591	336·0	135·0	173·0	1894·0
D-14	317·5	2·870	0·770	245·5	75·0	93·1	1920·2
W	229·0	2·231	0·758	131·0	108·3	94·3	1921·0
F	224·0	2·250	0·762	129·0	108·0	94·0	1921·0
D-15	110·0	1·328	0·860	96·7	53·2	110·0	1927·4
W	129·0	0·898	0·615	148·9	24·0	61·0	1939·5
F	129·0	0·951	0·611	149·0	25·2	61·0	1939·0
D-16	126·1	0·935	0·435	213·0	59·3	147·1	1894·5
W	120·0	0·975	0·418	149·7	118·2	145·6	1895·0
F	122·0	0·956	0·399	154·0	117·0	149·0	1894·0
D-17	154·5	0·783	0·387	316·7	34·2	0·6	1900·4
W	274·0	1·039	0·579	250·0	32·0	46·0	1896·2
F	267·0	1·013	0·567	243·0	31·2	53·0	1896·0
D-18							
W	88·0	0·278	0·653	12·3	57·3	146·4	1968·2
F	87·0	0·265	0·643	8·0	57·0	149·0	1968·0
D-19	423·5	1·330	0·700	60·1	73·7	71·1	1910·0
W	294·0	1·190	0·610	307·0	103·0	71·0	1912·8
F	288·0	1·151	0·620	305·0	102·9	71·0	1914·0
D-20	354·9	1·205	0·933	93·4	37·5	1·0	1887·3
W	510·0	1·424	0·886	352·0	122·0	98·0	1880·0
F	514·0	1·420	0·889	350·0	123·8	97·0	1880·0
D-21	321·0	2·120	0·188	159·0	47·8	87·9	1941·6
W	657·0	2·689	0·440	151·0	154·0	139·0	1866·0
F	626·0	2·540	0·406	152·0	164·0	138·0	1866·0
D-22	128·0	0·566	0·179	55·0	51·5	146·4	1946·7
W	178·0	0·688	0·081	41·2	129·4	152·2	1831·4
F	163·0	0·635	0·070	100·0	131·0	154·0	1951·0
D-23	151·7	0·695	0·375	59·7	67·4	167·8	1897·2
W	201·0	0·816	0·535	45·9	64·1	174·3	1897·0
F	199·0	0·834	0·522	45·0	64·8	175·1	1896·8
D-24	85·7	0·790	0·773	288·9	43·0	174·1	1904·7
W	97·0	0·743	0·770	287·0	27·0	177·0	1905·3
F	96·0	0·722	0·769	287·0	23·0	177·0	1905·0
D-25	40·8	0·500	0·350	114·2	69·7	119·1	1915·4
W	217·0	0·879	0·630	148·0	128·0	147·0	1903·0
F	264·0	0·885	0·656	148·0	128·0	145·0	1903·0

TABLE II

A comparison of the calculated dynamical parallaxes of the 25 Dyson binary stars utilizing the orbital elements given in Dyson's catalogue[1] *(D), the Washington Double Star Catalogue*[16] *(W), and the* FITASTROMETRY *program (F) optimized values of the 25 Dyson binary-orbit parameters. P is in years, a in arcseconds. The two values of parallax $\pi(H)$ and $\pi(G)$ are in milliarcseconds (mas) and are taken from the Hipparcos catalogue*[17] *(H) and from the Gaia catalogue*[6] *(G). Note that the Gaia catalogue did not have values for several of the binary systems. The dynamical parallaxes are calculated using the formula*

$$\pi_d = \frac{1000a}{P^{\frac{2}{3}}(M_1 + M_2)^{\frac{1}{3}}},$$

which is equation 52 in Chapter 14 of Smart[7]*, where π_d is in milliarcseconds, a is in arcseconds, P is in Besselian years, and the masses are in solar masses. The masses were estimated from the spectral classes of the two stars when they were available in the literature. If only the spectral class of one star was known, then $M_1 + M_2$ was replaced with 2·0 solar masses in accordance with Smart*[7]*.*

	P	a	$M_1 + M_2$	M $(2M_\odot)$	π_d	$\pi(H)$	$\pi(G)$
D-1	124·2	0·970	2·10		30·43	26·33	23·31
W	167·4	0·984	2·10		25·30	26·33	23·31
F	168·6	1·014	2·10		25·95	26·33	23·31
D-2	167·4	0·974	3·01		22·21	25·26	24·00
W	145·4	0·890	3·01		22·29	25·26	24·00
F	145·0	0·844	3·01		1·18	25·26	24·00
D-3	216·9	0·407		2·00	8·95	7·60	5·50
W	522·2	0·625		2·00	7·65	7·60	5·50
F	495·0	0·619		2·00	7·85	7·60	5·50
D-4	95·2	0·440		2·00	16·75	9·85	
W	188·0	0·549		2·00	13·28	9·85	
F	189·0	0·568		2·00	13·69	9·85	
D-5	88·2	0·627		2·00	25·12	24·56	22·67
W	98·0	0·743		2·00	27·74	24·56	22·67
F	94·0	0·751		2·00	28·83	24·56	22·67
D-6	59·6	0·350		2·00	18·21	16·14	
W	58·0	0·343		2·00	18·17	16·14	
F	57·0	0·326		2·00	17·47	16·14	
D-7	110·1	0·319		2·00	11·02	6·41	
W	104·6	0·329		2·00	11·76	6·41	
F	105·0	0·353		2·00	12·59	6·41	
D-8	361·0	1·000	3·24		13·33	11·08	11·81
W	421·0	1·071	3·24		12·89	11·08	11·81
F	486·0	1·130	3·24		12·35	11·08	11·81
D-9	220·4	1·205	3·56		21·63	16·42	17·72
W	245·0	1·111	3·56		18·58	16·42	17·72
F	242·0	1·005	3·56		16·95	16·42	17·72
D-10	193·6	2·549	1·48		66·84	74·58	74·09
W	156·0	2·443	1·48		73·98	74·58	74·09
F	157·0	2·438	1·48		73·51	74·58	74·09

TABLE II (*concluded*)

	P	a	$M_1 + M_2$	M $(2M_\odot)$	π_d	$\pi(H)$	$\pi(G)$
D-11	238·0	1·060	2·17		21·32	23·14	22·77
W	253·0	1·111	2·17		21·45	23·14	22·77
F	250·0	1·100	2·17		21·41	23·14	22·77
D-12	88·5	0·330		2·00	13·19	11·93	
W	89·0	0·327		2·00	13·02	11·93	
F	89·0	0·315		2·00	12·54	11·93	
D-13	234·8	1·271	2·80		23·69	28·93	26·58
W	257·0	1·450	2·80		25·45	28·93	26·58
F	261·0	1·466	2·80		25·47	28·93	26·58
D-14	317·5	2·870	1·63		52·40	50·87	51·74
W	229·0	2·231	1·63		50·65	50·87	51·74
F	224·0	2·250	1·63		51·83	50·87	51·74
D-15	110·0	1·328	4·52		34·99	18·84	
W	129·0	0·898	4·52		21·27	18·84	
F	129·0	0·951	4·52		22·53	18·84	
D-16	126·1	0·935		2·00	29·51	37·00	
W	120·0	0·975		2·00	31·81	37·00	
F	122·0	0·956		2·00	30·85	37·00	
D-17	154·5	0·783	2·51		20·01	17·12	15·74
W	274·0	1·039	2·51		18·12	17·12	15·74
F	267·0	1·013	2·51		17·98	17·12	15·74
D-18							
W	88·0	0·278		2·00	11·15	11·58	
F	87·0	0·265		2·00	10·71	11·58	
D-19	423·5	1·330		2·00	18·72	18·25	
W	294·0	1·190		2·00	21·36	18·25	
F	288·0	1·151		2·00	20·95	18·25	
D-20	354·9	1·205		2·00	19·08	15·50	16·32
W	510·0	1·424		2·00	17·71	15·50	16·32
F	514·0	1·420		2·00	17·56	15·50	16·32
D-21	321·0	2·120	4·37		27·66	19·77	21·15
W	657·0	2·689	4·37		21·76	19·77	21·15
F	626·0	2·540	4·37		21·23	19·77	21·15
D-22	128·0	0·566	2·73		15·94	15·70	
W	178·0	0·688	2·73		15·56	15·70	
F	163·0	0·635	2·73		15·23	15·70	
D-23	151·7	0·695	2·56		17·86	16·47	16·51
W	201·0	0·816	2·56		17·38	16·47	16·51
F	199·0	0·834	2·56		17·89	16·47	16·51
D-24	85·7	0·790	1·66		34·32	31·20	30·55
W	97·0	0·743	1·66		29·72	31·20	30·55
F	96·0	0·722	1·66		29·08	31·20	30·55
D-25	40·8	0·500	1·81		34·62	20·15	20·03
W	217·0	0·879	1·81		19·97	20·15	20·03
F	264·0	0·885	1·81		17·65	20·15	20·03

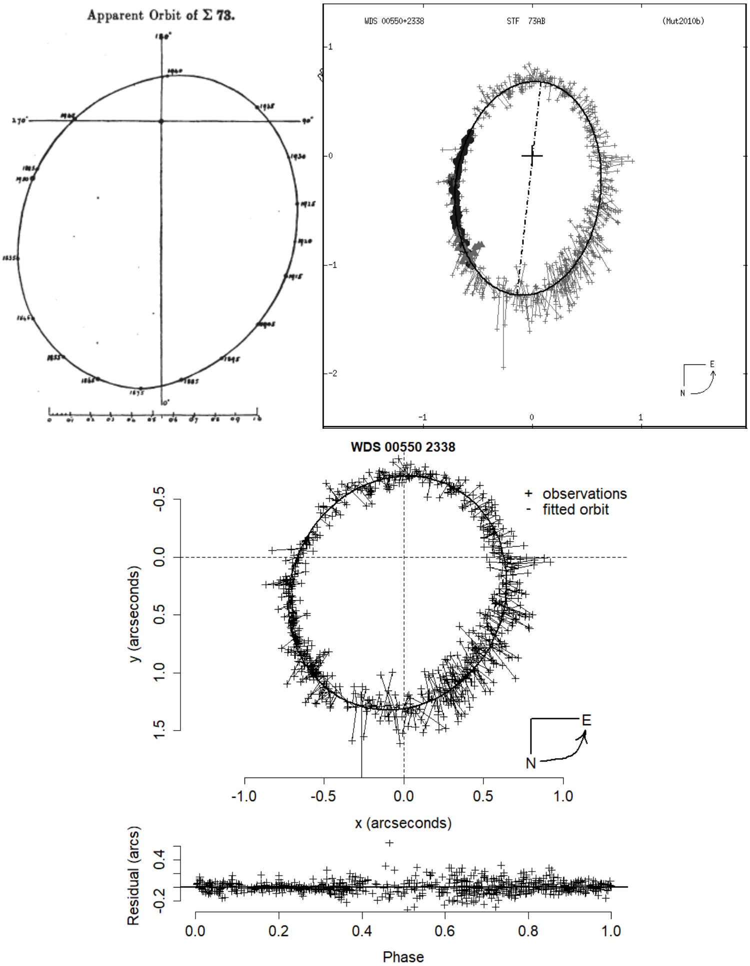

FIGS. 1, 2, AND 3

Orbital plots of WDS 00550+2338 from Dyson (1), WDS (2), and FITASTROMETRY (3) for comparison. The lower panel shows the residuals for the orbit immediately above it.

This highlights the potential problem that an ambiguity in the optimized solution can arise if the data set covers only a fraction of the total orbital period and/or if there is an appreciable scatter in the data set. Two other binary systems (2 and 17) exhibited the same difficulty. The optimized solutions of these other two systems are also found in the on-line appendix at: https://michaelrhodesbyu.weebly.com.

TABLE III

Results of the astrometric fittings of WDS 00550+2338. The three methods are Dyson (D), WDS (W), and FITASTROMETRY (F). P is in years, a in arcseconds, ω, i, and Ω are in degrees, and T_0 is in decimal tropical years AD. χ^2/n is the normalized χ^2 goodness of fit measure, where n is the number of observations. Δl is the recalculated error estimate, where the initial error estimate is multiplied by the term $\sqrt{\chi^2/n}$.

	P	a	e	ω	i	Ω	T_0	χ^2	χ^2/n	Δl
D	124·20	0·97	0·708	76·5	41·2	105·7	1815·93			
W	167·510	0·9837	0·306	358·62	44·57	173·66	1956·2			
F	168·6 ± 0·3	1·014 ± 0·003	0·308 ± 0·002	358·6 ± 0·6	45·2 ± 0·3	173·8 ± 0·4	1956·3 ± 0·2	2695	3·7	0·1

TABLE IV

Statistical coefficients of determination (R^2) for all 25 Dyson binary systems by fitted parameter comparing the WDS values to those derived by FITASTROMETRY, WDS to Dyson, and then WDS to adjusted Dyson in turn. P is in years, a in arcseconds, ω, i, and Ω are in degrees.

Parameter	*WDS to FITASTROMETRY*	*WDS to Dyson*	*WDS to adjusted Dyson*	*Linear regression gradient (WDS to FITASTROMETRY)*
ω	0·99	0·07	0·76	0·971 ± 0·021
i	0·99	0·00	0·53	1·102 ± 0·022
Ω	0·92	0·50	0·51	0·945 ± 0·059
P	0·98	0·85	0·85	0·991 ± 0·025
a	0·99	0·95	0·84	0·987 ± 0·006
e	0·99	0·50	0·50	1·022 ± 0·014

TABLE V

Fitting results for the WDS (W) and FITASTROMETRY (F) methods for the system WDS 00550+2338, where the initial parameter values P, a, e, ω, i, Ω, and T_0 were taken from the Dyson (D) fit. The Dyson parameter values are given for easy reference. P is in years. a is in arcseconds. ω, i, and Ω are in degrees. T_0 is in decimal tropical years AD.

	P	a	e	ω	i	Ω	T_0	χ^2	χ^2/n	Δl
D	124·20	0·97	0·708	76·5	41·2	105·7	1815·93			
W	167·510	0·9837	0·306	358·62	44·57	173·66	1956·2	1574		
F	116 ± 8	1·0 ± 0·2	0·75 ± 0·09	73 ± 9	43 ± 13	106 ± 10	1817 ± 5	83	3·0	0·09

TABLE VI

Fitting results for the FITASTROMETRY (F) method for the system WDS 00550+2338, where the initial parameter values P, a, e, ω, i, Ω, and T_0 were taken from the WDS (W) fit. Units and measures are the same as in Table V. The WDS and Dyson (D) optimal parameter values are given for reference.

	P	a	e	ω	i	Ω	T_0	χ^2	χ^2/n	Δl
D	124·20	0·97	0·708	76·5	41·2	105·7	1815·93			
W	167·510	0·9837	0·306	358·62	44·57	173·66	1956·2			
F	170 ± 60	1·0 ± 0·3	0·3 ± 0·3	358 ± 9	46 ± 16	172 ± 10	1954 ± 20	89	3·0	0·1

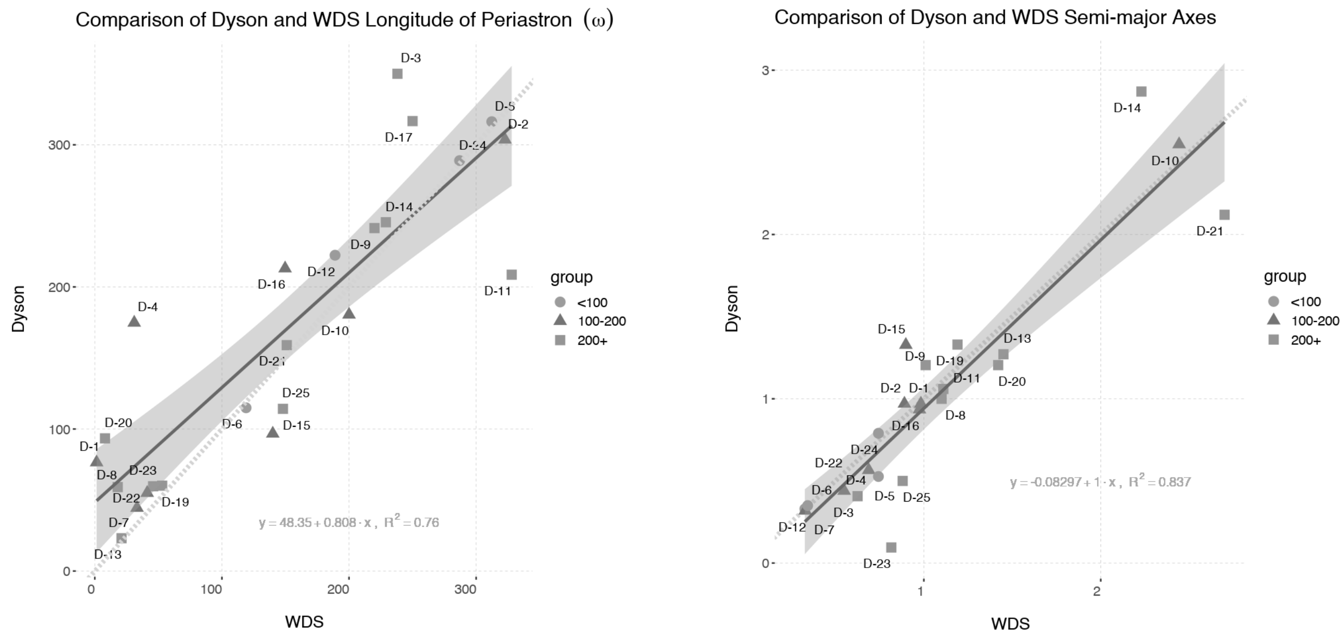

Fig. 4

The left-hand chart is a comparison of the longitude of periastron (ω, in degrees) estimates of the Dyson solutions *versus* those of WDS, while the right-hand chart compares the Dyson semi-major axis estimates (a, arcseconds) against those from WDS. The WDS solution used all available data to the current day. Systems have been classed into three groups based on their WDS periods.

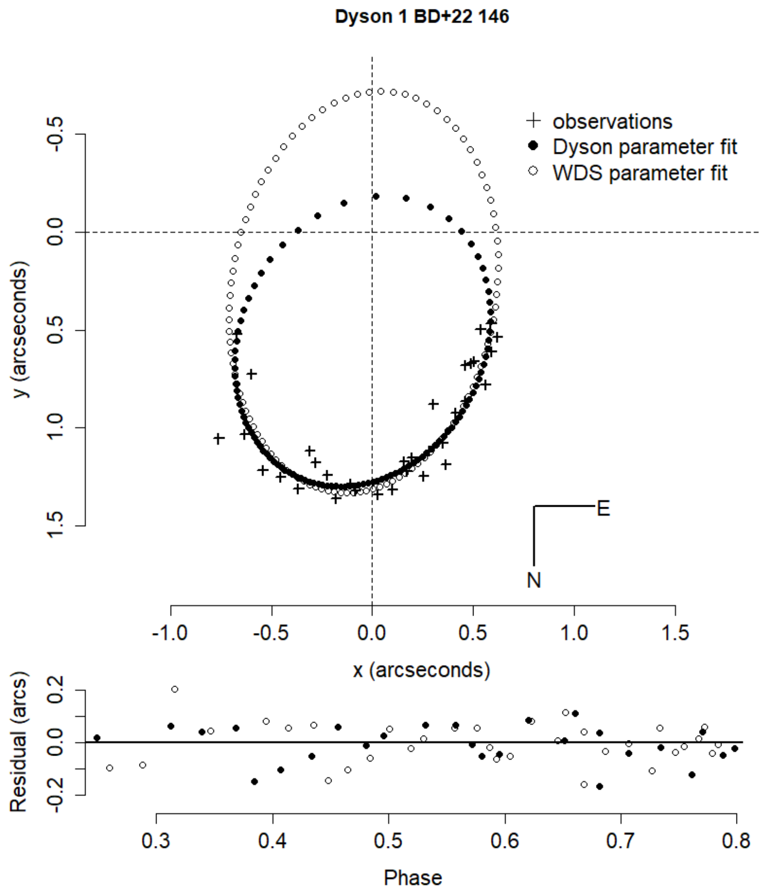

FIG. 5

Plots of FITASTROMETRY model apparent orbits of WDS 00550+2338 (BD+22 146, 36 And) comparing the curve obtained using Dyson or WDS values of the orbital parameters as starting values.

Conclusions

The main findings from our analysis of the 25 datasets in Dyson's (1921) catalogue can be summarized as follows:

(*i*) There is a good general agreement between the parameters of WDS and FITASTROMETRY when applied to the fuller WDS datasets, confirming that FITASTROMETRY's optimization algorithm performs satisfactorily where the prior parameters are not far from optimal. Such agreement has given us confidence to apply FITASTROMETRY to the previously unmodelled system V410 Pup[18], and to make this facility part of our 'analysis toolkit' for future systems.

(*ii*) The degree of agreement between the results of Dyson and later findings reflects the quantity and quality of available data. In this connection, the issue of local minima in the (χ^2, $\boldsymbol{a}$) hyperspace manifests itself, giving rise to alternative best-fit parameters, particularly with incomplete coverage or scattered data.

(*iii*) If the data set only covers a fraction of the complete orbit or there is significant scatter, FitAstrometry can often find at least two good model fits, depending on the choice of priors. This does not occur if the dataset covers a complete orbit and, as expected with more recent data, the scatter is low.

(*iv*) The analysis of 36 And, concentrated on in this presentation, allows a few general inferences. Thus, we found from fitting the Dyson datasets that, starting from their adopted priors in either case, both the Dyson and WDS posterior parameters were compatible, although the latter have large uncertainties and approach a 'long valley' with a noticeable $\omega - \Omega$ correlation. In fact, the sum $\omega + \Omega \approx 170°$ is about the same for either result. This can be understood, as for small i the two angles merge into one — the position angle of the major axis of a near face-on orbit. The large error estimates of the WDS posteriors at the cessation of iterations are associated with a decline in convexity of the (χ^2, $\boldsymbol{a}$) hypersurface. Numerical procedures become less accurate as the divisors become small, while the value of χ^2 hardly changes through many iterations. Although the angular parameters from the two fittings are markedly different, there is better consistency in the mass-related quantities, particularly a, the semi-major axis in arcseconds (Table III).

Acknowledgements

This research has made use of the *Washington Double Star Catalogue* maintained at the U.S. Naval Observatory. We thank Prof. Talar Yontan for discussion on *Gaia* and *Hipparcos* measurements.

References

(1) F. W. Dyson, *Catalogue of Double Stars* (H.M. Stationery Office, London), 1921.
(2) W. Herschel, *Phil. Trans. Royal Soc.*, **93**, 339, 1803.
(3) N. Shatsky & A. Tokovinin, *A&A*, **382**, 92, 2002.
(4) S. Söderhjelm, *A&A*, **341**, 121, 1999.
(5) M. A. Al-Wardat *et al.*, *PASA*, **38**, 2002.
(6) DR3, *A&A*, **674**, A1, 2023.
(7) W. M. Smart, *Textbook on Spherical Astronomy, 6th Edition* (Cambridge University Press), 1977.
(8) I. Ribas, F. Arenou & E. F. Guinan, *AJ*, **123**, 2002.
(9) I. J. D. Craig & J. C. Brown, *Inverse Problems in Astronomy, A guide to inversion strategies for remotely sensed data* (CRC Press), 1986.
(10) E. Budding & O. Demircan, *A Guide to Close Binary Systems* (CRC Press), 2022.
(11) W. H. Press *et al.*, *Numerical Recipes: The Art of Scientific Computing* (Cambridge University Press) 1986, p. 523.
(12) P. R. Adby & M. A. Dempster, *Introduction to Optimization Methods*, (Chapman and Hall Limited) 1974, p. 204.
(13) P. R. Bevington, *Data reduction and error analysis for the physical sciences* (McGraw-Hill), 1969, p. 228.
(14) E. Budding & O. Demircan, *loc. cit.*, 2022, ch. 5.
(15) J. Jackson, *MNRAS*, **80**, 543, 1920.
(16) B. D. Mason, G. L. Wycoff & W. I. Hartkopf, *The Washington Double Star Catalogue*, 2022.
(17) M. A. C. Perryman *et al.*, *The Hipparcos Catalogue*, *A&A*, **323**, L49, 1997.
(18) A. Erdem *et al.*, *MNRAS*, **515**, 6151, 2022.